JACS
JOURNAL OF THE AMERICAN CHEMICAL SOCIETY
Communication
pubs.acs.org/JACS

Spectroscopic Identification of an Fe^{III} Center, not Fe^{IV}, in the Crystalline Sc–O–Fe Adduct Derived from $[Fe^{IV}(O)(TMC)]^{2+}$

Jai Prakash,[†] Gregory T. Rohde,[†] Katlyn K. Meier,[‡] Andrew J. Jasniewski,[†] Katherine M. Van Heuvelen,[†,#] Eckard Münck,*[,‡] and Lawrence Que, Jr.*[,†]

[†]Department of Chemistry and Center for Metals in Biocatalysis, University of Minnesota, Minneapolis, Minnesota 55455, United States

[‡]Department of Chemistry, Carnegie Mellon University, Pittsburgh, Pennsylvania 15213, United States

Supporting Information

ABSTRACT: The apparent Sc^{3+} adduct of $[Fe^{IV}(O)(TMC)]^{2+}$ (**1**, TMC = 1,4,8,11-tetramethyl-1,4,8,11-tetraazacyclotetradecane) has been synthesized in amounts sufficient to allow its characterization by various spectroscopic techniques. Contrary to the earlier assignment of a +4 oxidation state for the iron center of **1**, we establish that **1** has a high-spin iron(III) center based on its Mössbauer and EPR spectra and its quantitative reduction by 1 equiv of ferrocene to $[Fe^{II}(TMC)]^{2+}$. Thus, **1** is best described as a Sc^{III}–O–Fe^{III} complex, in agreement with previous DFT calculations (Swart, M. *Chem. Commun.* **2013**, *49*, 6650.). These results shed light on the interaction of Lewis acids with high-valent metal-oxo species.

The role of redox-inactive Lewis-acidic metal ions in modulating the chemistry of redox-active metal-oxo centers has recently attracted considerable attention due to the requirement for a Ca^{2+} or Sr^{2+} ion to be an integral part of the oxygen evolving Mn_4O_5 cluster of photosystem II.[1−3] Seminal efforts of Agapie have addressed how the binding of Lewis acidic metal ions can affect properties of manganese-oxo clusters,[4−6] while complementary investigations of Fukuzumi and Nam have demonstrated the significant acceleration (by up to 8 orders of magnitude in some cases) of various oxidative transformations carried out by Fe^{IV}=O complexes upon addition of Lewis acidic metal ions, particularly Sc^{3+}.[7,8] Sc^{3+} binding has also been shown to facilitate trapping high-valent metal-oxo and imido complexes of late first row transition metal ions,[9−11] and heterobimetallic complexes with M^{III}–(μ-OH)–M^{II} cores (M^{III} = Fe, Mn, Ga; M^{II} = Ca, Sr, and Ba) have also been structurally characterized.[12]

An exciting development was the report of a crystal structure of the Sc^{3+}-bound $[Fe^{IV}(O)(TMC)]^{2+}$ adduct (TMC = 1,4,8,11-tetramethyl-1,4,8,11-tetraazacyclotetradecane) by Fukuzumi and Nam in 2010,[13] which provided the first crystallographic evidence for Sc^{3+} binding to an $Fe^{IV}(O)$ moiety and formulated the adduct as the neutral $[(TMC)(Fe^{IV}–O–Sc^{III})(OTf)_4(OH)]$ complex (**1**). However, scrutiny of the crystallographic data led to some concern about the iron(IV) oxidation state assignment.[14] Specifically, the observed average Fe–N_{TMC} bond length of 2.18 Å was 0.08 Å longer than that found in the crystal structure of the bona fide $[Fe^{IV}(O)(TMC)(NCMe)]^{2+}$ complex.[15] Additionally, the observed Sc–O bond length of 2.19 Å was more typical of Sc–OH_2 than Sc–OH distances.[16] These discrepancies prompted Swart to carry out DFT calculations to investigate the oxidation state of the Fe atom.[14] An iron(III) oxidation state was required to reproduce the metal–ligand bond lengths found in the crystal structure, leading Swart to conclude that the adduct should instead be formulated as $[(TMC)Fe^{III}–O–Sc^{III}(OTf)_4(OH_2)]$.

Although there are obviously methods for ascertaining iron oxidation state, **1** has only been characterized by X-ray crystallography. We surmised that the absence of additional data to characterize this intriguing complex was probably due to a lack of sufficient material, so we embarked on an effort to obtain larger amounts of the complex. Via a modification of the preparation method, we were able to obtain the desired adduct in about 50% yield, an amount sufficient to carry out characterization of the complex by Mössbauer and X-ray absorption spectroscopy of the crystals as well as electrospray ionization mass spectrometry and EPR spectroscopy of the solutions obtained from these crystals. Taken together, our studies establish the iron center in the adduct to be high-spin Fe(III). We thus confirm Swart's formulation of adduct **1** as $[(TMC)Fe^{III}–O–Sc^{III}(OTf)_4(OH_2)]$.

Our attempts to obtain larger amounts of **1** led us to make a small modification of the procedure reported by Fukuzumi et al.[13] and afforded a structural analogue of the target complex, designated **1a**, in which the apical water-derived Sc^{3+} ligand was replaced by MeCN (Figure 1). Instead of PhIO, 2-(^{t}BuSO_2)-C_6H_4IO (ArIO dissolved in trifluoroethanol)[17] was used as oxidant in the synthetic procedure, resulting in a dramatic increase in the yield of these crystals to ∼50%. Upon reaction of $Fe^{II}(TMC)(OTf)_2$ with ArIO, the characteristic blue-green chromophore of the oxoiron(IV) complex was obtained as expected. Subsequent addition of 1 equiv of $ScOTf_3$ elicited no immediate change in the near-IR band of the Fe^{IV}=O precursor, but the solution turned yellow over the course of a week, during which time yellow crystals of **1a** were obtained by vapor diffusion of Et_2O into the reaction solution at −20 °C. The crystals of **1a** used for spectroscopic analysis were harvested by decanting off most of the mother liquor followed

Received: January 16, 2015
Published: March 6, 2015

DOI: 10.1021/jacs.5b00535
J. Am. Chem. Soc. 2015, 137, 3478−3481

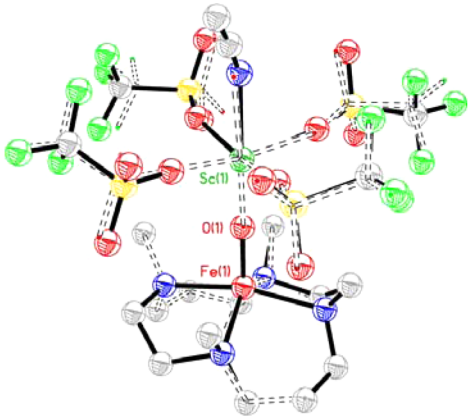

Figure 1. Overlay of X-ray structures of **1a** (solid lines) and **1** (dashed lines). For clarity, the atoms of **1a** were drawn as spheres to the 25% probability level and the atoms of **1** were drawn as small dots. Hydrogen atoms were omitted in both structures. The rmsd between the Sc, μ-O, Fe, and all non-hydrogen TMC atoms was found to be 0.0742 Å and is illustrated by the small deviation in bonds drawn above. The crystallographic R-factor (R_1) is 0.0791, and complete XRD experimental and refinement details are reported in the SI.

by carefully removing the remaining mother liquor with tissues; the crystals were then washed quickly with cold diethyl ether and dried under vacuum at −20 °C. In addition to X-ray crystallography, we were able to characterize **1a** in the solid state by X-ray absorption and Mössbauer spectroscopy, and in MeCN solution by EPR, ICP-MS, and ESI-MS techniques.

X-ray analysis of the crystals of **1a** confirmed the earlier structure reported by Fukuzumi et al.,[13] except for the replacement of the water-derived ligand on the Sc^{3+} in **1** by CH_3CN in **1a**. Despite this change, the crystallographic parameters (Figure S1 and Tables S1A and S1B) obtained for the (N4)Fe−O−Sc$(OTf)_4$ core are essentially identical, a conclusion illustrated by the overlay of the two structures (Figure 1). The root-mean-square deviation (rmsd, calculated by OFIT SHELX) for the overlay of the equivalent atoms in the two structures, namely Sc, μ-O, Fe, and all non-hydrogen atoms of the TMC macrocycle, is remarkably small at 0.0742 Å. As previously noted, the oxo bridge is coordinated *syn* to the TMC methyl groups, opposite to the *anti* configuration found for $[Fe^{IV}(O)(TMC)(NCMe)]^{2+}$.[15a] Importantly, key bond distances are in close agreement, such as the Fe−O distances of 1.748(5) Å for **1a** and 1.753(3) Å for **1** and an average Fe−N_{TMC} distance of 2.167(6) Å for **1a** and 2.175(3) Å for **1**. The Fe−O bond lengths are typical of 5-coordinate Fe^{III}−O−Fe^{III} complexes,[18] while the Fe−N_{TMC} distances are associated with Fe^{III}(TMC) complexes.[19−21] Importantly, the apical CH_3CN ligand in **1a** removes the ambiguity of assigning the iron oxidation state based solely on the presence or absence of protons on the solvent-derived apical ligand, which is not advisable with X-ray diffraction experiments. Indeed, two triflate oxygen atoms in the structure of **1** are found at appropriate distances to act as hydrogen bond acceptors for the water-derived ligand in **1** (Figure S2), supporting its assignment as a neutral aqua species, rather than a hydroxide as proposed in ref 13.

Fe K-edge X-ray absorption spectroscopic studies were also performed on a solid sample of **1a**. The Fe K-edge of **1a** is observed at 7122.6 eV (Figure S3), which falls within the range of known high-spin Fe(III) species.[20,22−24] Moreover, there is a pre-edge peak at 7114.3 eV (Figure 2 inset) with an area of 32

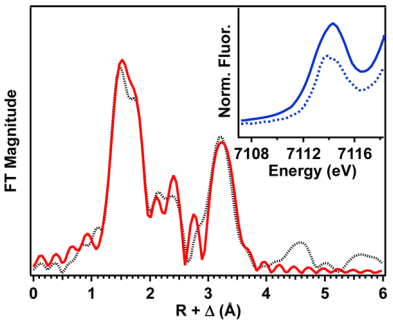

Figure 2. Fourier transform of the Fe K-edge EXAFS data for **1a** over a k range of 2−14.5 $Å^{-1}$ (the black dotted line is experimental data; the solid red line is the best fit with one O scatterer at 1.74 Å, four N scatterers at 2.17 Å, and one Sc scatterer at 3.69 Å). The inset compares the pre-edge features of **1a** (solid line) and $[Fe^{III}(\eta^1$-OOH)(TMC)$]^{2+}$ (dotted line).

units, which is by far the largest pre-edge area known for any 5- or 6-coordinate high-spin Fe(III) species in the literature.[20,22−24] This large area indicates a high degree of distortion from centrosymmetry upon scandium binding, reflecting the square-pyramidal geometry around the iron(III) ion that moves the Fe 0.53 Å away from the mean N4-plane of the TMC framework. Although not as large as **1a**, the pre-edge areas of related $[Fe^{III}(TMC)(\eta^1$-OOH)$]^{2+}$ (**2**) and $[Fe^{III}(TMC)(\eta^2$-$O_2)]^{+}$ (**3**) complexes are also quite large (22.4 and 17.9 units, respectively),[20] reflecting the large differences between the bond lengths Fe−N_{TMC} (∼2.2 Å) and Fe−O (1.74 Å for **1a**, 1.92 Å for **2**, and 1.93 Å for **3**) and the number of O ligands. An EXAFS analysis was performed on this solid sample to ensure that the bulk solid contained the same material as the single crystal of **1a**. Fits of the EXAFS region (Figures 2 and S4 and Table S2) revealed four N scatterers at 2.17 Å, one O scatterer at 1.74 Å, and one Sc scatterer at 3.69 Å, in excellent agreement with the X-ray structure. Importantly, the Sc scatterer in this sample exhibits a much more prominent feature in the Fourier-transformed data than in the spectrum of the Sc^{3+} adduct of $[Fe^{III}(TMC)(\eta^2$-$O_2)]^{+}$.[20b,21]

In order to gain insight into the iron oxidation state, we have studied Mössbauer and EPR spectra of **1a**. Mössbauer spectra of crystals of **1a** were collected at 4.2 K in parallel applied magnetic fields, **B**, up to 7.5 T. For **B** < 2 T the spectra were found to be broadened due to spin−spin interactions between neighboring molecules in the crystals. For **B** > 4 T, however, the applied field sufficiently decouples these interactions so that well-resolved spectra were obtained. The spectra shown in Figure 3 unambiguously show that **1a** is a high-spin ferric complex. The red lines in Figure 3 are spectral simulations based on the $S = 5/2$ spin Hamiltonian,

$$H = D\left[S_z^2 - \frac{35}{12} + \left(\frac{E}{D}\right)(S_x^2 - S_y^2)\right] + g_0\beta\vec{S}\cdot\vec{B} + A_0\vec{S}\cdot\vec{I} - g_n\beta_n\vec{B}\cdot\vec{I} + H_Q$$

where

$$H_Q = \frac{eQV_{zz}}{12}\left[3I_z^2 - \frac{15}{4} + \eta(I_x^2 - I_y^2)\right]$$

and all symbols have their conventional meanings; the parameters used are listed in the caption of Figure 3. The salient features of the spectra are as follows. Complex **1a** has an

DOI: 10.1021/jacs.5b00535
J. Am. Chem. Soc. 2015, 137, 3478−3481

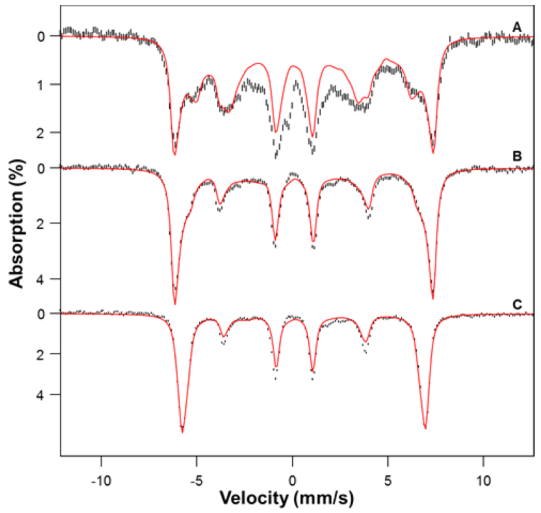

Figure 3. 4.2 K Mössbauer spectra of crystals of **1a** recorded in parallel applied fields of 1.0 (A), 4.0 (B), and 7.5 T (C). From spectral simulations using an $S = 5/2$ spin Hamiltonian, we obtained $D = 3.25$ cm^{-1}, $E/D = 0.14(2)$, $g_0 = 2.00$, $A_0/g_n\beta_n = -19.1(2)$ T, $\Delta E_Q = -1.02(5)$ mm s^{-1}, $\eta \approx 0$, and $\delta = 0.36(3)$ mm s^{-1}. We have subtracted from the data a spectral simulation for two Fe^{IV}═O contaminants (representing 8% of Fe), namely $[Fe^{IV}(O)(TMC)(NCMe)]^{2+}$ (5%) and $[Fe^{IV}(O)(TMC)(OH)]^{+}$ (3%), using the parameters reported in ref 15.

isomer shift $\delta = 0.36(3)$ mm s^{-1} and a quadrupole splitting $\Delta E_Q = -1.02(5)$ mm s^{-1}, and the major component of the electric field gradient tensor is negative ($\Delta E_Q < 0$). The δ and ΔE_Q values agree within the experimental uncertainty with respective values of 0.39(5) and −0.99(50) mm s^{-1} from DFT calculations of Swart who postulated **1** to be a high-spin ferric complex.[14] The ^{57}Fe **A**-tensor of **1a** is isotropic as expected for high-spin Fe^{III}. The zero-field splitting parameter $D \approx +3$–4 cm^{-1} was determined from the intensities of the nuclear $\Delta m = 0$ transitions (lines 2 and 5 counting from the left). The rhombicity parameter E/D was determined as follows. The splitting between the outermost lines of the **B** = 1.0 T spectrum reflects the internal magnetic field, $\mathbf{B}_{int} = \langle S_y \rangle A_0/g_n\beta_n$, associated with the ground Kramers doublet. The expectation value of $\langle S_y \rangle$, like the effective g-value $g_{eff,y}$ of the doublet, depends sensitively on E/D ($\langle S_y \rangle = -g_{eff,y}/4$ for $\beta\mathbf{B}/D \ll 1$ for the spin-down level). With A_0 known from the 4.0 and 8.0 T spectra (which are quite insensitive to E/D along the critical y direction), the magnetic splitting of the 1.0 T spectrum can be used to determine E/D. We found $E/D = 0.14 \pm 0.02$, in excellent agreement with the EPR value $E/D = 0.14$ obtained for **1a** dissolved in MeCN (see below), showing that both in the solid state and in frozen solution **1a** has a high-spin Fe^{III} site, with the same structure. At least 90% of the iron in the sample can be attributed to **1a**; the sample contains two Fe^{IV}═O contaminants (see Figure 3 caption), estimated to represent ∼8% of the Fe in the sample.

The findings obtained by Mössbauer spectroscopy are fully corroborated by the EPR spectra of **1a** obtained in frozen MeCN solution (Figure 4), which display resonances arising from two Kramers doublets of a high-spin Fe^{III} system with $D > 0$ and $E/D = 0.14$. A simulation of the whole spectrum (red) is shown in Figure 4, together with a simulation (blue) of the signal associated with the first excited Kramers doublet. The ground Kramers doublet of **1a** gives rise to a signal with effective g-values at $g_{eff} = (2.87, 8.57, 1.48)$, the intensities of

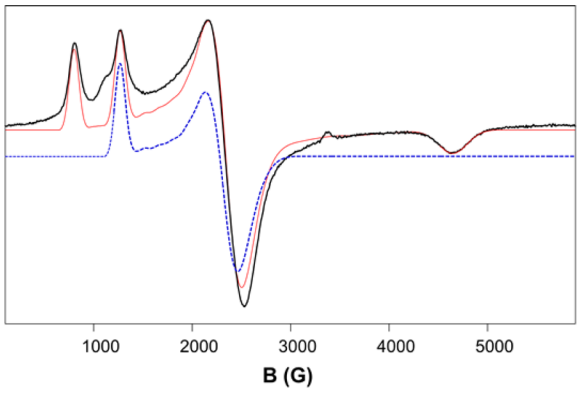

Figure 4. X-band EPR spectrum (black trace) of **1a** in MeCN. The red line is a SpinCount simulation using $D = 3.25$ cm^{-1}, $E/D = 0.14$, and $g_0 = 2.00$. Two of the Kramers doublets of the high-spin iron(III) center contribute to the spectrum. For $E/D = 0.14$ the ground doublet has $g_{eff} = (2.87, 8.57, 1.48)$, while the spectrum of the middle doublet has $g_{eff} = (3.00, 2.64, 5.4)$ (dashed blue line, offset for clarity). The upper doublet would yield a very weak resonance (not seen) at $g_{eff} = 9.95$. Conditions: $T = 30$ K; microwave power, 20 μW; modulation amplitude, 1 mT.

which increase as the temperature is decreased from 30 to 2 K (Figure S5). Concomitantly, the intensity of the $g_{eff} = (3.00, 2.64, 5.4)$ signal decreases, which assigns this feature as the g_{max} signal of the middle Kramers doublet. Some features of the EPR spectrum of **1a** are worth noting. First, the sample lacks a signal at $g = 4.3$ often associated with rhombic Fe^{III}. Second, complex **1a** is one of the rare examples of a high-spin Fe^{III} species with intermediate E/D for which all of the expected signals from the ground Kramers doublet are clearly resolved. Finally, the EPR results establish that the iron center has a +3 oxidation state in solution.

We have characterized other properties of **1a** in MeCN solution. Consistent with the assignment of an iron(III) oxidation state for **1a**, its electronic absorption spectrum (Figure S6) did not exhibit the NIR feature characteristic of $[Fe^{IV}(O)(TMC)(NCMe)]^{2+}$ ($\lambda_{max} = 824$ nm).[15] The only feature observed was an intense UV band at $\lambda_{max} = 307$ nm ($\varepsilon = 9500$ M^{-1} cm^{-1}) that is likely associated with the Fe−O−Sc unit of **1a**. Low-temperature ESI-MS analysis showed a prominent ion cluster peak at $m/z = 820$ and an associated isotope pattern corresponding to the formulation $[(TMC)(Fe)(O)(Sc)(OTf)_3]^{+}$ (Figure 5), confirming the persistence of the solid state structure in solution. There was also a less intense peak at $m/z = 478$ corresponding to the $[(TMC)(Fe)(OH)(OTf)]^{+}$ ion, presumably due to a small amount of

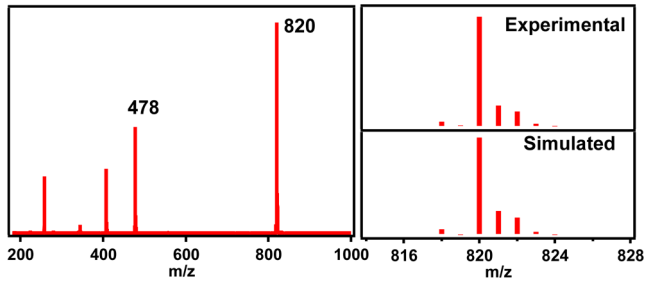

Figure 5. ESI-MS spectrum of **1a** crystals dissolved in MeCN obtained by injecting the solution at −30 °C into the mass spectrometer preset at a low dry gas temperature of 25 °C.

DOI: 10.1021/jacs.5b00535
J. Am. Chem. Soc. 2015, 137, 3478−3481

hydrolysis of **1a** under the experimental conditions. An ICP-MS analysis of **1a** in MeCN solution revealed a Sc:Fe ratio of 0.9, consistent with the Mössbauer finding showing that **1a** represents 90% of the Fe in the bulk sample.

$[Fe^{IV}(O)(TMC)(NCMe)]^{2+}$ was previously shown to undergo 2-e$^-$ reduction by 2 equiv of ferrocene in the presence of Sc^{3+}.[13] In contrast, **1a** was reduced by only 1 equiv of ferrocene (even when excess ferrocene is used, Figure S7), affording $[Fe^{II}(TMC)]^{2+}$ quantitatively, as indicated by the quantitative formation of $[Fe^{IV}(O)(TMC)(NCMe)]^{2+}$ upon treating the ferrocene-reduced sample with PhIO. There was also a significant difference in the rates of ferrocene oxidation between $[Fe^{IV}(O)(TMC)(NCMe)]^{2+}$ and **1a**. At −20 °C, the oxidation of 1 equiv of ferrocene by $Fe^{IV}(O)(TMC)(NCMe)]^{2+}$ in the presence of 1 equiv of Sc^{3+} takes ∼4 h, but the corresponding reaction with **1a** was complete within 10 min, making **1a** 24-fold more reactive than $[Fe^{IV}(O)(TMC)(NCMe)]^{2+}$ in the presence of 1 equiv Sc^{3+}. These results also provide support for the assignment of a +3 oxidation state for the iron center in **1a.**

In summary, we have re-investigated the nature of the apparent Sc^{3+} adduct of $[Fe^{IV}(O)(TMC)]^{2+}$ [13] by obtaining sufficient amounts of the isolated complex to allow thorough spectroscopic investigation in both the solid state and in solution. Our studies conclusively establish that the iron center in **1a** is not iron(IV) as was previously assigned on the basis of X-ray crystallography data alone,[13] but is in fact in a high-spin iron(III) state as proposed by Swart.[14] This oxidation state assignment is also supported by the observation that only 1 equiv of ferrocene is required to reduce **1a** to $[Fe^{II}(TMC)]^{2+}$. We are actively pursuing studies to address important mechanistic questions regarding the identity of the 1-e$^-$ reductant that converts $[Fe^{IV}(O)(TMC)]^{2+}$ to **1a** upon Sc^{3+} binding and how the oxo atom becomes coordinated *syn* to the methyl groups on the TMC ligand.

■ ASSOCIATED CONTENT

Supporting Information

Experimental details, additional spectroscopic data, and a crystallographic file in CIF format for **1a**. This material is available free of charge via the Internet at http://pubs.acs.org.

■ AUTHOR INFORMATION

Corresponding Authors

*emunck@cmu.edu

*larryque@umn.edu

Present Address

[#]K.M.V.H.: Department of Chemistry, Harvey Mudd College, Claremont, CA 91711, United States

Notes

The authors declare no competing financial interest.

■ ACKNOWLEDGMENTS

This work was supported by grants from the NSF (CHE-1361773 to L.Q. and CHE-1305111 to E.M.). We thank the University of Minnesota for a dissertation fellowship to G.T.R. and the NIH for a postdoctoral fellowship (GM-093479) to K.M.V.H. XAS data were collected on beamline X3B at the National Synchrotron Radiation Lightsource, which is supported by the U.S. Department of Energy under Contract No. DE-AC02-98CH10886. Use of beamline X3B was made possible by the Center for Synchrotron Biosciences grant, P30-EB-00998, from the National Institute of Biomedical Imaging and Bioengineering. Lastly, we thank Prof. M. Swart and Dr. Victor G. Young, Jr. for valuable discussions.

■ REFERENCES

(1) Yano, J.; Yachandra, V. *Chem. Rev.* **2014**, *114*, 4175.

(2) Umena, Y.; Kawakami, K.; Shen, J.-R.; Kamiya, N. *Nature* **2011**, *473*, 55.

(3) Rivalta, I.; Brudvig, G. W.; Batista, V. S. *Curr. Opin. Chem. Biol.* **2012**, *16*, 11.

(4) Kanady, J. S.; Tsui, E. Y.; Day, M. W.; Agapie, T. *Science* **2011**, *333*, 733.

(5) Tsui, E. Y.; Tran, R.; Yano, J.; Agapie, T. *Nat. Chem.* **2013**, *5*, 293.

(6) Tsui, E. Y.; Agapie, T. *Proc. Natl. Acad. Sci. U.S.A.* **2013**, *110*, 10084.

(7) Fukuzumi, S. *Coord. Chem. Rev.* **2013**, *257*, 1564.

(8) Park, J.; Morimoto, Y.; Lee, Y.-M.; Nam, W.; Fukuzumi, S. *Inorg. Chem.* **2014**, *53*, 3618.

(9) Chen, J.; Lee, Y.-M.; Davis, K. M.; Wu, X.; Seo, M. S.; Cho, K.-B.; Yoon, H.; Park, Y. J.; Fukuzumi, S.; Pushkar, Y. N.; Nam, W. *J. Am. Chem. Soc.* **2013**, *135*, 6388.

(10) (a) Pfaff, F. F.; Kundu, S.; Risch, M.; Pandian, S.; Heims, F.; Pryjomska-Ray, I.; Haack, P.; Metzinger, R.; Bill, E.; Dau, H.; Comba, P.; Ray, K. *Angew. Chem., Int. Ed.* **2011**, *50*, 1711. (b) Kundu, S.; Miceli, E.; Farquhar, E.; Pfaff, F. F.; Kuhlmann, U.; Hildebrandt, P.; Braun, B.; Greco, C.; Ray, K. *J. Am. Chem. Soc.* **2012**, *134*, 14710.

(11) Hong, S.; Pfaff, F. F.; Kwon, E.; Wang, Y.; Seo, M.-S.; Bill, E.; Ray, K.; Nam, W. *Angew. Chem., Int. Ed.* **2014**, *53*, 10403.

(12) (a) Lacy, D. C.; Park, Y. J.; Ziller, J. W.; Yano, J.; Borovik, A. S. *J. Am. Chem. Soc.* **2012**, *134*, 17526. (b) Park, Y. J.; Cook, S. A.; Sickerman, N. S.; Sano, Y.; Ziller, J. W.; Borovik, A. S. *Chem. Sci.* **2013**, *4*, 717.

(13) Fukuzumi, S.; Morimoto, Y.; Kotani, H.; Naumov, P.; Lee, Y.-M.; Nam, W. *Nat. Chem.* **2010**, *2*, 756.

(14) Swart, M. *Chem. Commun.* **2013**, *49*, 6650.

(15) (a) Rohde, J.-U.; In, J.-H.; Lim, M. H.; Brennessel, W. W.; Bukowski, M. R.; Stubna, A.; Münck, E.; Nam, W.; Que, L., Jr. *Science* **2003**, *299*, 1037. (b) Jackson, T. A.; Rohde, J.-U.; Seo, M. S.; Sastri, C. V.; DeHont, R.; Stubna, A.; Ohta, T.; Kitagawa, T.; Münck, E.; Nam, W.; Que, L., Jr. *J. Am. Chem. Soc.* **2008**, *130*, 12394.

(16) Meehan, P. R.; Aris, D. R.; Willey, G. R. *Coord. Chem. Rev.* **1999**, *181*, 121.

(17) Macikenas, D.; Skrzypczak-Jankun, E.; Protasiewicz, J. D. *J. Am. Chem. Soc.* **1999**, *121*, 7164.

(18) Kurtz, D. M., Jr. *Chem. Rev.* **1990**, *90*, 585.

(19) Cho, J.; Jeon, S.; Wilson, S. A.; Liu, L. V.; Kang, E. A.; Braymer, J. J.; Lim, M. H.; Hedman, B.; Hodgson, K. O.; Valentine, J. S.; Solomon, E. I.; Nam, W. *Nature* **2011**, *478*, 502.

(20) (a) Li, F.; Meier, K. K.; Cranswick, M. A.; Chakrabarti, M.; Van Heuvelen, K. M.; Münck, E.; Que, L., Jr. *J. Am. Chem. Soc.* **2011**, *133*, 7256. (b) Li, F.; Van Heuvelen, K. M.; Meier, K. K.; Münck, E.; Que, L., Jr. *J. Am. Chem. Soc.* **2013**, *135*, 10198.

(21) Lee, Y.-M.; Bang, S.; Kim, Y. M.; Cho, J.; Hong, S.; Nomura, T.; Ogura, T.; Troeppner, O.; Ivanovic-Burmazovic, I.; Sarangi, R.; Fukuzumi, S.; Nam, W. *Chem. Sci.* **2013**, *4*, 3917.

(22) (a) Shan, X.; Rohde, J.-U.; Koehntop, K. D.; Zhou, Y.; Bukowski, M. R.; Costas, M.; Fujisawa, K.; Que, L., Jr. *Inorg. Chem.* **2007**, *46*, 8410. (b) Koehntop, K. D.; Rohde, J.-U.; Costas, M.; Que, L., Jr. *Dalton Trans.* **2004**, 3191.

(23) Westre, T. E.; Kennepohl, P.; DeWitt, J. G.; Hedman, B.; Hodgson, K. O.; Solomon, E. I. *J. Am. Chem. Soc.* **1997**, *119*, 6297.

(24) Roe, A. L.; Schneider, D. J.; Mayer, R. J.; Pyrz, J. W.; Widom, J.; Que, L., Jr. *J. Am. Chem. Soc.* **1984**, *106*, 1676.

DOI: 10.1021/jacs.5b00535
J. Am. Chem. Soc. 2015, 137, 3478−3481